

RESEARCH ARTICLE

Open Access



Seasonal variation, source identification, and health risk assessment of atmospheric polycyclic aromatic hydrocarbons (PAHs) in Ulsan, South Korea

Na Ra Youn^{1†}, Sang-Jin Lee^{1†}, Tuyet Nam Thi Nguyen^{1,2}, Ho-Young Lee¹, Hye Kyung Cho¹, Chang-Keun Song^{1,3} and Sung-Deuk Choi^{1,3*} 

Abstract

Gaseous and particulate 21 PAHs were monitored at a residential site in Ulsan, South Korea, over three seasons (December 2013–August 2014). The mean concentrations of Σ_{21} PAHs were highest in winter (16.2 ± 8.2 ng/m³), followed by spring (8.37 ± 4.53 ng/m³) and summer (6.23 ± 2.53 ng/m³). The mean gaseous concentration of Σ_{21} PAHs (7.39 ± 4.39 ng/m³) was 2.7 times higher than that of particulate PAHs (2.70 ± 3.38 ng/m³). To identify the sources of PAHs (both types of sources and their areas), diagnostic ratios, principal component analysis, and concentration-weighted trajectory (CWT) were used. The results showed that pyrogenic sources (e.g., coal combustion) were the primary emission sources of PAHs in winter and spring. In summer, the influence of both coal and heavy oil combustion was dominant, suggesting that PAHs could be transported from industrial areas of Ulsan (e.g., petrochemical and nonferrous industrial complexes) by seasonal winds. Regarding emission source areas, the CWT analysis revealed that in winter and spring, PAHs in Ulsan could be attributed to emissions from regional areas, e.g., China and North Korea. The PAH concentrations were also used to assess the health risks associated with the inhalation of these compounds for adults aged 18–70. The results showed that the cancer risks from Σ_{19} PAHs and Σ_{13} PAHs did not exceed the guideline set by the US EPA (10^{-6}), indicating no cancer risks for this target group. However, it is worth noting that certain PAHs, which are not listed as priority PAHs by the US EPA, make significant contributions to the benzo[a]pyrene equivalent and the associated cancer risks. Therefore, it is necessary to investigate not only the priority PAHs but also other PAH species to fully evaluate their effect on human health.

Keywords PAHs, Ulsan, Seasonal variation, Source identification, Risk assessment

[†]Na Ra Youn and Sang-Jin Lee contributed equally to this work as co-first authors.

*Correspondence:
Sung-Deuk Choi
sdchoi@unist.ac.kr

Full list of author information is available at the end of the article

1 Introduction

Polycyclic aromatic hydrocarbons (PAHs), a group of chemicals with two or more benzene rings composed of carbon and hydrogen in their structure, have been extensively studied due to their potential carcinogenic, teratogenic, and mutagenic properties (IARC, 2010). Based on their frequent detection, carcinogenicity, and mutagenicity, the United States Environmental Protection Agency (US EPA) has classified 16 PAHs as priority pollutants: naphthalene (Nap), acenaphthylene (Acy), acenaphthene (Ace), fluorene (Flu), phenanthrene (Phe), anthracene (Ant), fluoranthene (Flt), pyrene (Pyr), benzo[a]anthracene (BaA), chrysene (Chr), benzo[b]fluoranthene (BbF), benzo[k]fluoranthene (BkF), benzo[a]pyrene (BaP), indeno[1,2,3-c,d]pyrene (IcdP), dibenzo[a,h]anthracene (DahA), and benzo[g,h,i]perylene (BghiP). Some US EPA 16 priority PAHs, such as BaP, Chr, BbF, BkF, BaA, IcdP, and DahA, are classified as human carcinogens or possible carcinogens (IARC, 2010). However, despite their high toxicity, some PAHs have not been listed as the priority PAHs (e.g., dibenz[a,l]pyrene (DbalP), benzo[c]phenanthrene (BcPhe), benzo[j]fluoranthene (BjF), dibenz[a,i]pyrene (DbaiP), and dibenz[a,h]pyrene (DbahP)). Notably, these compounds have been regarded as possible human carcinogens (IARC, 2010); thus, an investigation of the occurrence of these chemicals in the environment and human health risks is essential.

To estimate the detrimental health effects resulting from exposure to PAHs, the toxicity equivalency factor (TEF) methodology was developed (Nisbet and Lagoy, 1992; US EPA, 1993) and has been widely used. The TEF presents the relative toxicity of individual PAHs compared to BaP, which has been well characterized toxicologically. The evaluation of toxicity for the 16 US EPA priority PAHs is well established, while studies for the toxicity of other PAHs are limited (Andersson and Achten, 2015). For example, DbalP, DbaiP, and DbahP have been reported to have a carcinogenic potential about 10 times greater than that of BaP (Andersson and Achten, 2015; OEHHA, 1994). In addition, 7,12-dimethylbenz[a]anthracene (DMBA) and 3-methylcholanthrene (3MCA) have potencies 21.8 and 1.9 times greater in laboratory animals than BaP (Collins et al., 1998; OEHHA, 1994). However, environmental monitoring studies on these non-US EPA priority PAHs have been limited.

As PAHs are semi-volatile organic compounds, they typically exist in both particulate and gaseous phases after being emitted from combustion processes (e.g., biomass and fossil fuel burning) (Mostert et al., 2010), as well as from petrogenic sources (e.g., oil spillages or leakages) (Silva and Bicego, 2010). Considering their major sources and human exposure, atmospheric monitoring

of PAHs has been predominantly conducted in urban and industrial areas. Even though they have high toxicity, the ambient monitoring of non-US EPA priority PAHs has been limited. Recently, several studies reported the atmospheric levels of DbalP, DbaiP, DbahP, 3MCA, and DMBA; they were generally detected at low concentrations even in industrial cities (Hong et al., 2023; Kirchsteiger et al., 2023; Ray et al., 2019).

In South Korea, atmospheric levels of PAHs and their impact on human health have been significant concerns, particularly in industrial cities (Baek et al., 2020a; Baek et al., 2020c; Thang et al., 2019). Among the megacities in South Korea, Ulsan is the largest multi-industrial city located in the southeastern part of the Korean Peninsula, housing petrochemical, nonferrous, automobile, and shipbuilding industrial complexes. Due to the proximity of residential areas to these industrial complexes, residents are highly expected to be exposed to PAHs emitted from industrial activities (Nguyen et al., 2020). The levels of PAHs and their human exposure in Ulsan are significantly affected by seasonal wind patterns (Choi et al., 2012b; Nguyen et al., 2018). For example, PAH concentrations are highest in winter due to increased fossil fuel combustion for residential heating and long-range atmospheric transport (LRAT). Furthermore, summer exhibits low levels of PAHs, but the influence of industrial emissions increases due to southeasterly seasonal winds. Regarding target compounds, only one study reported the particulate concentrations of non-US EPA priority PAHs and their health risk in Ulsan (Baek et al., 2020b). However, this previous study did not investigate seasonal variations, gas/particle partitioning, potential sources, and LRAT of PAHs.

In this study, the seasonal concentrations, profiles, and phase distribution of 21 PAHs, including non-US EPA priority PAHs with high toxicity, were investigated in Ulsan. Besides, source types and source areas of PAHs were identified seasonally. Finally, cancer risks induced by exposure to the 21 PAHs via inhalation were calculated.

2 Materials and methods

2.1 Air sample collection

Air samples were collected at the rooftop of the Yeongnam intensive air monitoring station (YN station) (35°34′52.36″N, 129°19′27.15″E), which is located in a residential area north and northwest of urban and industrial areas in Ulsan (Fig. 1). Sampling was conducted over three seasons, from December 2013 to August 2014, excluding fall since winter and summer best reflect the highest and lowest emissions of primary pollutants, respectively. Additionally, winter and summer are characterized by enhanced LRAT and local emission effects, respectively (Lee et al., 2023a; Nguyen et al., 2022).



Fig. 1 Locations of industrial areas and the sampling site (YN station) in Ulsan, South Korea

Furthermore, during the spring season, the LRAT of PAHs associated with particulate matter can be increased by Asian dust events (Choi et al., 2012a).

A high-volume air sampler (HV-700E, Sibata, Japan) was used to collect gaseous and particulate samples once a week for 24 h, resulting in a total of 64 samples collected during the sampling period. The air volume for each sample was 1007.9 m³ (flow rate: 700 L/min). Gaseous and particulate samples were collected on glass fiber filters (GFFs, 203 mm × 254 mm, Advantec, Japan) and two polyurethane foam plugs (PUFs, diameter 90 mm × height 50 mm, Ziemer Chromatographie, Germany), respectively.

Before sampling, GFFs were baked at 400 °C for 4 h to remove organic contaminants, and PUFs were sonicated for 30 min with acetone and n-hexane, respectively. After sampling, the GFFs and PUFs were stored at −9 °C, wrapped in aluminum foil and placed in polyurethane zippered bags until analysis.

2.2 Analytical procedure

Prior to extraction, a surrogate standard mixture of Nap-d₈, Ace-d₁₀, Phe-d₁₀, Chr-d₁₂, and Per-d₁₂ (Z-014J, AccuStandard Inc., USA) was added to all samples. PAHs collected on the GFFs and PUFs were extracted using Soxhlet extractors for 20 h with 350 mL of n-hexane/acetone (9:1). The extracts were concentrated to 10 mL using a TurvoVap II (Caliper, USA) and then cleaned up on a

silica gel column containing 2 g of anhydrous sodium sulfate, 5 g of activated silica gel (4 h at 130 °C), and 2 g of anhydrous sodium sulfate with 70 mL of n-hexane/dichloromethane (9:1). The effluents were concentrated to 0.5 mL using the TurvoVap (Classic II, Biotage, Sweden) and a nitrogen evaporator (MG-2200, Eyela, Japan). These final extracts were transferred to gas chromatography (GC) vials, and then an internal standard of p-terphenyl-d₁₄ (M525-FS-2, AccuStandard Inc., USA) was added to the vial prior to instrumental analysis.

Among the 16 US EPA priority PAHs, Nap, Acy, and Ace were excluded due to their low recoveries, potential sampling artifacts, and blank contamination. A gas chromatograph/mass spectrometer (GC/MS, 7890A/5975C, Agilent, USA) equipped with a DB-5MS capillary column (30 m × 0.25 mm i.d., 0.25-μm film thickness) was used for the analysis. The final sample (1 μL) was injected into the GC in splitless mode at an inlet temperature of 300 °C. The carrier gas was helium (He), with a flow rate of 1.0 mL/min. The GC oven temperature started at 60 °C for 1 min, increased at 10 °C/min until 320 °C, and finally held at 320 °C for 8 min. The MS was operated under selected ion monitoring (SIM) mode.

2.3 Quality assurance and quality control (QA/QC)

Field blank samples were collected to account for the contamination during all processes from sampling to analysis (e.g., fieldwork, shipping to the laboratory, storage,

pretreatment, and analysis). The concentrations of PAHs were corrected using average blank values ($n = 10$). Average recoveries of the PUF samples were 61%, 95%, and 85%, and those of the GFF samples were 78%, 99%, and 100% for Phe-d10, Chr-d12, and Per-d12, respectively. The method detection limits (MDLs) of gaseous and particulate individual PAHs were calculated using the following equation:

$$\text{MDL} = \text{SD} \times 3.14 \quad (1)$$

where SD indicates the standard deviation of 7 replicates of spiked blank samples, and 3.14 is the Student's t -value for a 99% confidence level. The MDLs ranged from 0.01 to 0.13 ng/m³ for gaseous samples and from 0.02 to 0.08 ng/m³ for particulate samples. PAH concentrations below the MDLs were treated as non-detects (NDs), which were substituted with half of the MDLs. If the target compound was not detected in any of the samples, it was excluded from statistical calculations. The MDLs and detection frequencies (%) of PAHs in gaseous and particulate samples are presented in Table S1 in the supplementary information. In addition, to confirm the reproducibility of the analytical method, the coefficient of variation (CV) for the seven MDL samples was calculated. The CVs for particulate and gaseous PAHs were determined to be 5.8% and 6.8%, respectively.

2.4 Identification of emission sources

2.4.1 Emission source types

The emission sources of PAHs were identified using principal component analysis (PCA). To mitigate detection limit artifacts (Choi et al., 2012b), only compounds with over a 50% detection frequency (Table S1) were considered as input data. Individual PAH concentrations were normalized by the total concentration of each sample. The rotation method for PCA was varimax, and eigenvalues greater than one were used for PC extraction. The analysis was conducted using IBM SPSS Statistics 20.0 (IBM Corp., USA). Additionally, four diagnostic ratios were applied to identify emission sources of PAHs: Flt/(Flt+Pyr), Flu/(Flu+Pyr), BaA/(BaA+Chr), and IcdP/(IcdP+BghiP). These ratios were calculated for individual samples, and the influence of pyrogenic and petrogenic sources (Yunker et al., 2002), petroleum combustion, and coal/wood/biomass burning (Akyuz and Cabuk, 2010; Yunker et al., 2002) was distinguished.

2.4.2 Identification of LRAT source areas

The concentration-weighted trajectory (CWT), a hybrid receptor model, was used to locate regional emission sources and LRAT. Backward air trajectories used for CWT were modeled using the Hybrid Single-Particle Lagrangian Integrated Trajectory (HYSPLIT) model

(<https://www.ready.noaa.gov/HYSPLIT.php>). The backward trajectories of 72 h were calculated every hour for each 24-h HiVol sample (from 11:00 AM local time). The starting height of trajectories was 500 m above the ground. A total of 768 trajectories (32 sampling days \times 24 h per day) were obtained for three seasons (i.e., winter, spring, and summer). The seasonal backward air trajectories are illustrated in Fig. S1 in the supplementary information.

The CWT assigns a weighted concentration of the target compound associating trajectories in each grid cell based on the below equation:

$$\text{CWT}_{ij} = \frac{1}{\sum_{l=1}^L \tau_{ijl}} \sum_{l=1}^L C_l \tau_{ijl} \quad (2)$$

where CWT_{ij} denotes the CWT value of the cell i, j . C_l is the PAH concentration, and L represents the total number of backward air trajectories. τ_{ijl} denotes the endpoint number of air trajectories in grid cell i, j (Hsu et al., 2003). TrajStat software (version 1.2.2.6) was used to calculate CWT values (Wang et al., 2009). The domain of CWT was 110–140°E and 25–50°N with the grid cell of 0.5° \times 0.5°. Areas with higher CWT values are expected to be source areas of PAHs. A weighted function $W(n_{ij})$, as described in Eq. (3), was used to reduce the trailing effect, which indicates the high uncertainty of source areas due to a small number of trajectories passing through grid cells (Stojic and Stojic, 2017).

$$W(n_{ij}) = \begin{cases} 1, & 2av \leq n \\ 0.75, & av \leq n < 2av \\ 0.5, & 0.5av \leq n < av \\ 0.25, & n < 0.5av \end{cases} \quad (3)$$

where n denotes the number of trajectory endpoints in each grid cell and av is the average number of trajectory endpoints per cell.

2.5 Health risk assessment

Human health risks via the inhalation of PAHs were calculated for adults (i.e., 18–70 years old). The concentration of individual PAHs was first converted to its BaP equivalent concentration (BaP_{eq}) using the following equation:

$$\text{BaP}_{\text{eq}} = C \times \text{TEF} \quad (4)$$

where BaP_{eq} denotes the BaP equivalent concentration of each PAH compound (ng/m³). C is the concentration of individual PAHs (ng/m³), and TEF represents the toxic equivalent factor. In previous studies, the cancer risk of PAH exposure was estimated using BaP_{eq} to consider the comprehensive risk of PAHs (Chen et al., 2017; Nisbet and Lagoy, 1992; Sun et al., 2015). The IARC

classification and TEFs for the target PAHs are listed in Table S2. Among the 21 PAHs, 19 were considered for health risk assessment because TEFs of BcPhe and BeP were not provided in the literature.

The incremental lifetime cancer risk (ILCR) model was used to calculate the potential carcinogen risk of the PAHs via inhalation using the following equation:

$$ILCR = (ISF \times BaP_{eq} \times IR \times EF \times ED \times cf) / (BW \times AT) \quad (5)$$

where ISF (mg/kg/day) is the inhalation slope factor, IR (m³/h) is the inhalation rate, and EF (day/year) and ED (year) denote the exposure frequency and exposure duration, respectively. cf (10⁻⁶) is the conversion factor. BW (kg) and AT (days) represent the body weight and averaging time, respectively. While the risk levels of PAH exposure through inhalation may vary by gender and age, the differences are considered insignificant compared to guideline levels (Nguyen et al., 2020). Thus, this study focused solely on adults. Details of the risk parameters are provided in Table S3. Monte Carlo simulation with 10,000 iterations was conducted using Crystal Ball 11.1 (Oracle, USA) to calculate the risk uncertainty.

3 Results and discussion

3.1 Pollution characteristics of PAHs

3.1.1 Levels and seasonal variations

The range and mean concentrations of PAHs in the gaseous, particulate, and total (gaseous + particulate) phases over the sampling period are presented in Table 1 and Fig. 2. The mean Σ₂₁ PAH concentrations were highest in winter (mean ± standard deviation: 16.2 ± 8.2 ng/m³), followed by spring (8.37 ± 4.53 ng/m³) and summer (6.23 ± 2.53 ng/m³). A statistically significant difference in concentrations between winter and summer was found (Mann-Whitney rank-sum test, *p* < 0.01). This seasonal trend was identical for both the gaseous (winter: 10.7 ± 4.8 ng/m³, spring: 6.27 ± 4.19 ng/m³, and summer: 5.53 ± 2.44 ng/m³) and particulate (winter: 5.58 ± 4.69 ng/m³, spring: 2.20 ± 1.53 ng/m³, and summer: 0.69 ± 0.42 ng/m³) PAHs and is in accordance with the seasonal variations in previous studies (Hong et al., 2020; Ichikawa et al., 2018; Nguyen et al., 2018; Vuong et al., 2020). The higher PAH concentrations in winter and spring can be attributed to an increase in fuel combustion for heating and LRAT

Table 1 Range and mean concentrations (ng/m³) of the gaseous, particulate, and total (gas + particle) PAHs for the entire sampling period in Ulsan

Ring no.	Compounds	Gas		Particle		Total	
		Range	Mean	Range	Conc.	Range	Mean
3	Flu	ND–6.69	1.30 ± 1.75	ND–0.04	0.01 ± 0.01	0.01–6.71	1.30 ± 1.75
3	Phe	0.37–7.69	3.69 ± 2.00	ND–0.79	0.10 ± 0.16	0.39–8.10	3.79 ± 2.07
3	Ant	ND–0.75	0.16 ± 0.17	ND–0.03	0.02 ± 0.02	0.01–0.78	0.17 ± 0.18
4	Flt	0.37–2.25	1.17 ± 0.57	ND–2.28	0.40 ± 0.60	0.45–4.04	1.57 ± 0.93
4	Pyr	0.21–2.54	0.97 ± 0.58	ND–1.77	0.32 ± 0.46	0.38–2.76	1.29 ± 0.69
4	BcPhe	< MDL*	0.01	ND–0.28	0.06 ± 0.07	0.04–0.29	0.07 ± 0.07
4	BaA	ND–0.11	0.01 ± 0.02	ND–0.60	0.10 ± 0.15	0.01–0.61	0.11 ± 0.14
4	Chr	ND–0.19	0.03 ± 0.05	ND–1.22	0.23 ± 0.31	0.04–1.23	0.26 ± 0.31
5	Bb+jF	< MDL*	0.01	ND–1.50	0.32 ± 0.20	0.02–1.50	0.32 ± 0.20
5	BkF	< MDL*	0.01	ND–0.72	0.16 ± 0.20	0.03–0.73	0.17 ± 0.20
4	DMBA	**	ND	**	ND	**	ND
5	BeP	< MDL*	0.01	ND–1.18	0.28 ± 0.33	0.02–1.19	0.29 ± 0.33
5	BaP	< MDL*	0.01	ND–0.56	0.13 ± 0.15	0.03–0.58	0.14 ± 0.15
5	3MCA	**	ND	**	ND	**	ND
6	IcdP	< MDL*	0.01	ND–1.20	0.27 ± 0.32	0.02–1.21	0.28 ± 0.32
5	DahA	< MDL*	0.00	ND–0.10	0.03 ± 0.02	ND–0.10	0.03 ± 0.02
6	BghiP	ND–0.22	0.01 ± 0.04	ND–1.01	0.27 ± 0.29	0.03–1.02	0.28 ± 0.29
6	DbaiP	**	ND	**	ND	**	ND
6	DbahP	< MDL*	0.00	ND–0.03	0.00 ± 0.01	ND–0.03	0.00 ± 0.01
6	DbaIP	**	ND	**	ND	**	ND
	Σ ₂₁ PAHs	1.46–17.6	7.39 ± 4.39	0.28–12.8	2.70 ± 3.38	1.84–29.7	10.1 ± 6.84

ND Non-detected

* For values below the method detection limits (< MDL), they have been replaced by MDL/2 for statistical calculation

** If the target compounds were not detected in all samples, MDL/2 was not applied, and these compounds were excluded from the statistical calculation

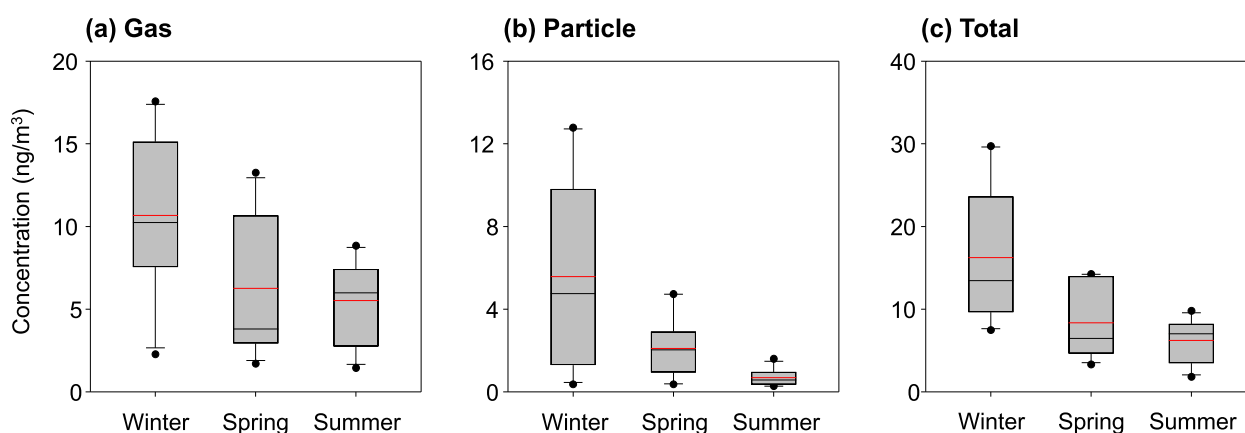


Fig. 2. Seasonal concentrations of the total Σ_{21} PAHs in **a** the gaseous, **b** particulate, and **c** total (gaseous + particulate) phases. The red line in the box is for a mean concentration

(Thang et al., 2019). The lowest PAH concentrations in summer would result from a substantial decrease in residential heating and photochemical reactions between PAHs and atmospheric oxidants under the conditions of high temperature and solar radiation (Baek et al., 1991; Nguyen et al., 2018).

The total (gas + particle) concentrations of Σ_{21} PAHs and the US EPA priority Σ_{13} PAHs in Ulsan and those in other residential areas in the world are presented in Table S4. The concentrations of Σ_{13} PAHs in this study (particle: 2.20 ng/m³, gas: 7.37 ng/m³, total: 9.57 ng/m³) were comparable to those reported in a previous study (particle: 2.55 ng/m³, gas: 4.11 ng/m³, total: 6.67 ng/m³) at a suburban site in Ulsan (Nguyen et al., 2018), while the concentration of particulate Σ_{13} PAH in Ulsan was lower than those in other Korean cities such as Seoul (8.42 ng/m³) (Kim et al., 2021), Incheon (12.2 ng/m³) (Kim et al., 2021), and Sihwa-Banwol (3.31 ng/m³) (Lee et al., 2023b). The concentration of particulate Σ_{21} PAHs observed in this study (2.70 ng/m³) was 1.4 and 2.1 times lower than those found in other Korean mega-cities, such as Gwangju (3.93 ng/m³) (NIER, 2018) and Daejeon (5.83 ng/m³) (NIER, 2019), respectively, whereas it was relatively similar to those in Yeongam, Korea (2.70 ng/m³) (NIER, 2016) and Chiba, and Japan (2.86 ng/m³) (Ichikawa et al., 2018). In addition, the total (gaseous + particulate) PAHs in this study (Σ_{21} PAHs: 10.1 ng/m³ and Σ_{13} PAHs: 9.57 ng/m³) were 1.5 times higher than those in Stockholm, Sweden (Σ_{21} PAHs: 6.44 ng/m³ and Σ_{13} PAHs: 6.24 ng/m³) (Masala et al., 2016) and Alberta, Canada (Σ_{21} PAHs: 6.57 ng/m³ and Σ_{13} PAHs: 6.13 ng/m³) (Hsu et al., 2015). The higher PAH concentrations in Ulsan might be attributed to local industrial emissions, especially from the petrochemical and nonferrous industrial complexes (Kwon and Choi, 2014). The emission

source types and source areas of the target PAHs are discussed more in Section 3.2.

3.1.2 Phase distributions and profiles

The mean gaseous Σ_{21} PAH concentration (7.39 ± 4.39 ng/m³) was 2.7 times higher than the particulate one (2.70 ± 3.38 ng/m³) (Mann-Whitney rank-sum test, $p < 0.01$). In general, the high mobility of gaseous PAHs, leading to their shorter half-lives than the particulate species, and the photochemical degradation during the transport of gaseous PAHs in the atmosphere can cause their lower levels at receptors (Ravindra et al., 2008). Additionally, the particulate PAH concentration was similar to or higher than that of gaseous PAHs at a background site in Jeju Island in Korea, mostly influenced by LRAT (Choi et al., 2012a). In contrast, in urban and industrial cities with large amounts of local emissions, gaseous PAH concentration is higher (Kim et al., 2012; Liu et al., 2014). Therefore, the higher concentrations of gaseous PAHs in this study were expected to be due to an effect of local emission sources.

For the gaseous phase, the 3-ring (69.5%) and 4-ring (29.7%) PAHs were predominant (Fig. 3), and strong correlations between the gaseous total PAHs and the 3- to 4-ring species were observed (Table S5), indicating that the behavior of gaseous PAHs is governed by the 3-ring PAHs and some 4-ring PAHs (e.g., Flt and Pyr) having relatively low molecular weights (< 203). The fractions of 3-ring PAHs (i.e., Flu, Phe, and Ant) increased in winter and spring compared to summer (Fig. 3), mostly due to increased emissions of PAHs from domestic heating in cold seasons (Thang et al., 2019).

The contribution of particulate PAHs was greatest in winter (34.3%), followed by spring (25.1%) and summer

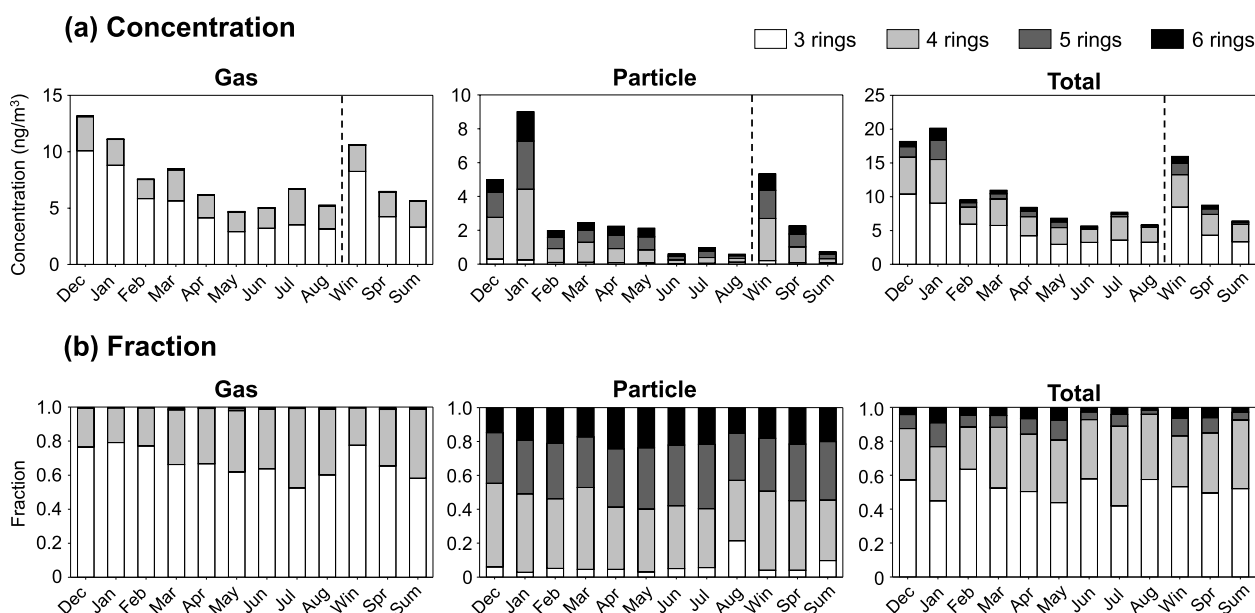


Fig. 3 Monthly and seasonal variations of the PAHs of ring number groups: **a** concentrations and **b** fractions in the gaseous, particulate, and total phases

(11.1%) (Fig. S2). In addition, the proportions of particulate PAHs in winter and spring were statistically higher than that in summer (Mann-Whitney rank-sum test, $p < 0.05$). The lowest proportions of particulate PAHs in summer can be attributed to a shift of particulate PAHs towards the gaseous phase due to the high temperature and sunlight intensity in summer (Esen et al., 2008; Kiss et al., 1998). Additionally, the greater fractions of particulate PAHs (i.e., 4- to 6-ring species) in winter and spring (Fig. S2) could be attributed to increased fossil fuel burning and higher concentrations of total suspended particles (TSP), which act as sorbents for PAHs, during these periods (winter: $94.8 \mu\text{g}/\text{m}^3$, spring: $145.7 \mu\text{g}/\text{m}^3$) compared to that in summer ($79.9 \mu\text{g}/\text{m}^3$).

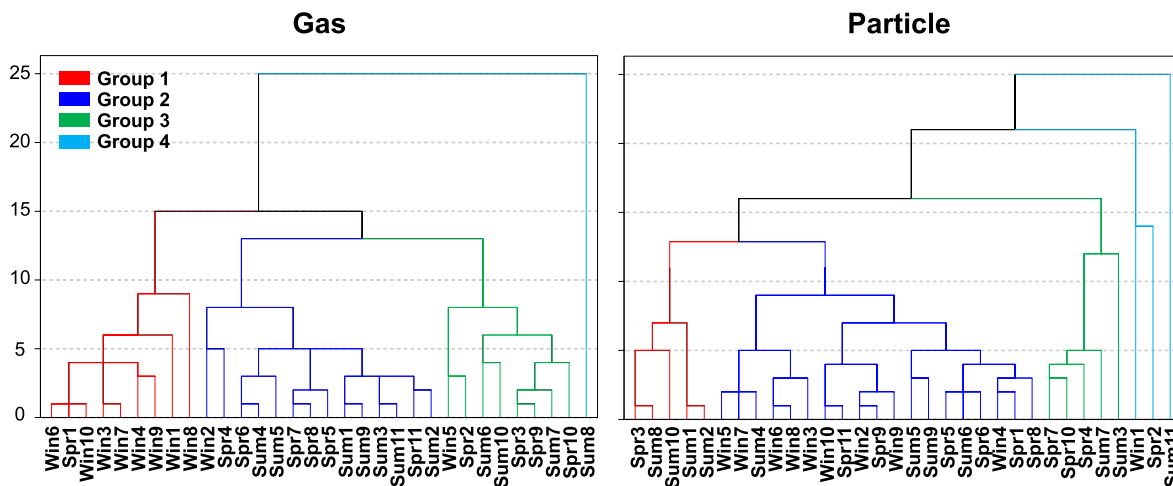
Regarding particulate distributions based on ring numbers, the 4-ring species (i.e., Flt, Pyr, and Chr) were the most abundant (41.7%), followed by the 5-, 6-, and 3-ring PAHs (33.3%, 20.3%, and 4.6%, respectively). A significant fraction of the 4- to 6-ring species (i.e., BaP, Ind, and BghiP) tends to associate with particulate matter due to their lower volatility and higher octanol-air partition coefficients (Baek et al., 1991), resulting in their predominant fractions in the particulate phase compared to other species (i.e., 3-ring PAHs). The strong correlations between particulate matter (TSP, PM_{10} , and $\text{PM}_{2.5}$) and the 4- to 6-ring PAHs (Table S5) support this discussion.

3.2 Source identification of PAHs

3.2.1 Identification of emission sources

The PCA results for gaseous and particulate PAHs in three seasons are depicted in Fig. 4. PC1 and PC2 accounted for 52.1% and 29.6% of the total variance, respectively. Both gaseous and particulate samples were classified into four groups by a dendrogram from the hierarchical cluster analysis (Fig. 4a). The gaseous samples of spring and summer were not separated, and many of them were classified into Groups 2 and 3 of the score plot of PCA (Fig. 4b), suggesting that gaseous PAHs in these seasons were affected by similar emission sources. Group 2 samples were characterized by a high loading of Phe, a marker for gasoline and/or diesel emissions from vehicles (Cheruiyot et al., 2015; Kulkarni and Venkataraman, 2000). Group 3 samples were characterized by Flt and Pyr, associated with coal combustion (Ravindra et al., 2008; Simcik et al., 1999). Winter samples were well separated from other seasons, exhibiting strong loadings of Flu and Ant (Fig. 4b), which are mainly derived from coal combustion (Simcik et al., 1999). Diagnostic ratios (Fig. 5) also confirmed that most samples were dominantly influenced by pyrogenic sources. In particular, winter samples were more affected by solid fuel burning, reflecting increased domestic heating, while petroleum combustion (e.g., vehicle emissions) was more important in spring and summer (Fig. 5a). Furthermore, it appears that winter samples were more influenced by diesel

(a) Dendrogram



(b) PCA

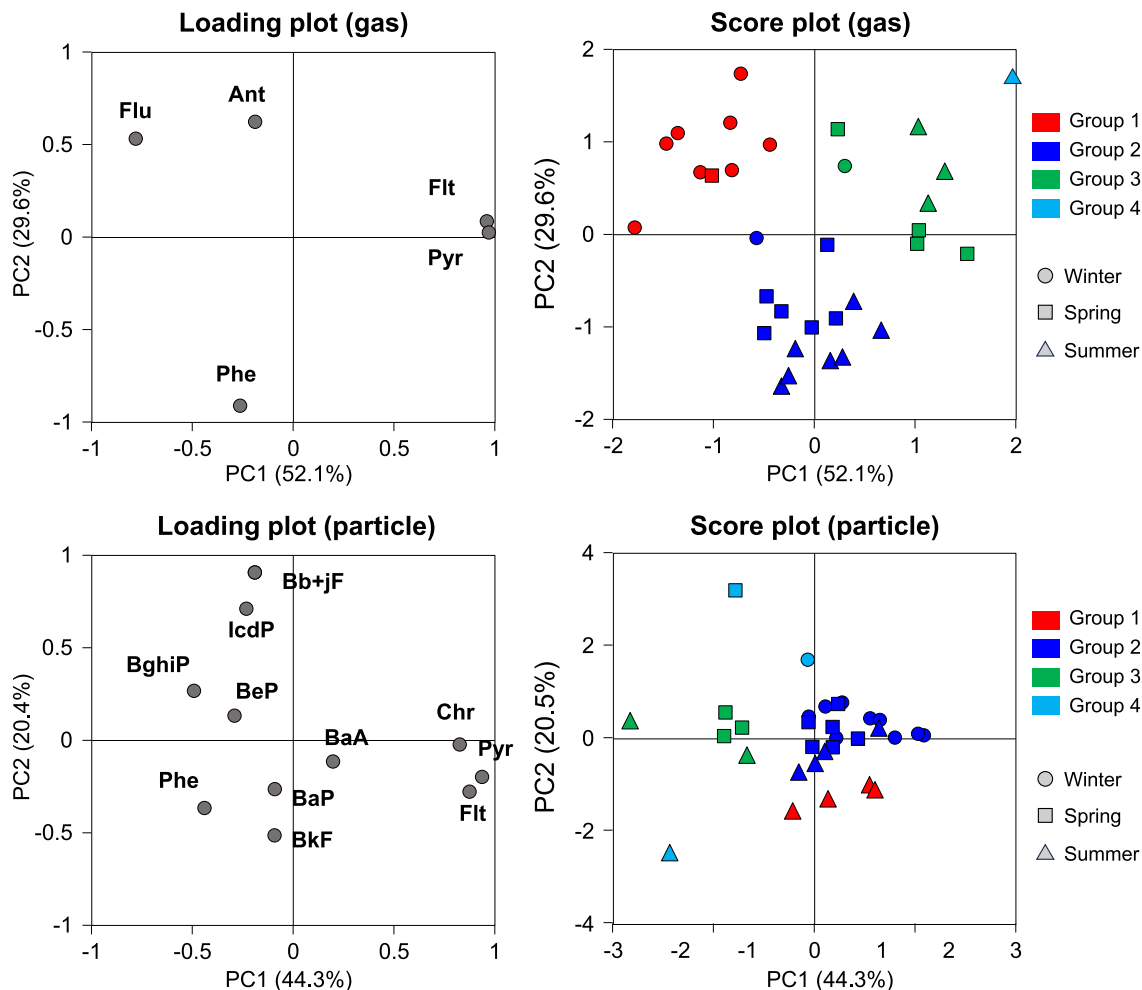


Fig. 4 Groups of gaseous and particulate samples classified using **a** hierarchical cluster analysis and **b** PCA results, including score and loading plots for the samples and PAH compounds, respectively

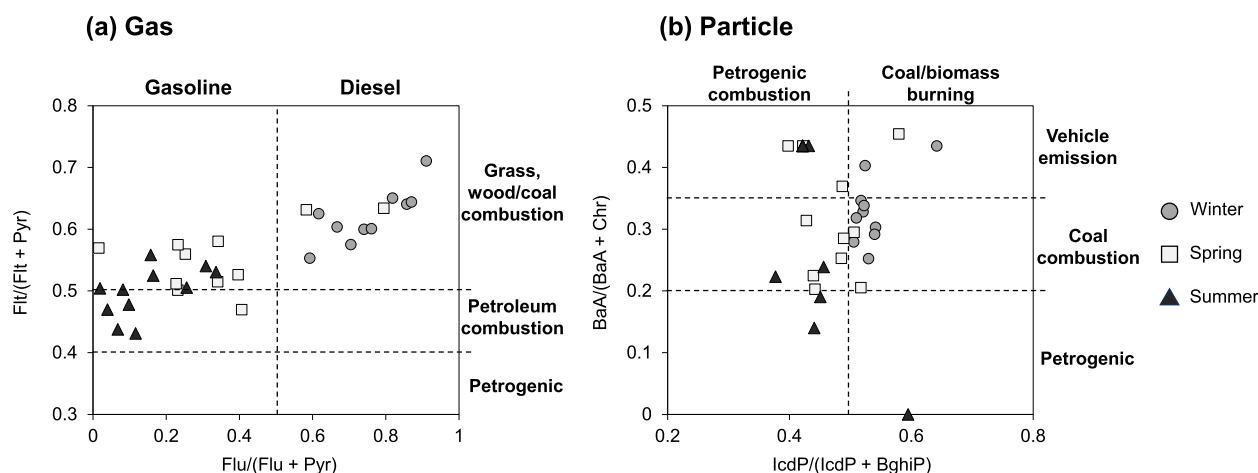


Fig. 5 Diagnostic ratios of PAHs in **a** the gaseous and **b** particulate phases: **a** $Ft/(Ft + Pyr)$ versus $Flu/(Flu + Pyr)$ and **b** $IcdP/(IcdP + BghiP)$ versus $BaA/(BaA + Chr)$

combustion rather than gasoline combustion, attributed to diesel engines operating at lower temperatures in cold weather, leading to incomplete combustion and increased PAH formation (Tang et al., 2005).

For the particulate samples, PC1 and PC2 accounted for 44.3% and 20.4% of the total variance, respectively (Fig. 4c). Winter samples were mostly located in Group 2 and characterized by Ft, Pyr, Chr, BaA, and BaP. Among these compounds, BaA and BaP are typical tracers for gasoline and diesel exhausts (Andrade et al., 2010; Harkov and Greenberg, 1985), while Ft, Pyr, and Chr are known to be significantly emitted from coal combustion (Ravindra et al., 2008; Simcik et al., 1999). Thus, particulate PAHs in winter were possibly derived from both vehicle emissions and coal combustion. Diagnostic ratios (Fig. 5b) also suggest that coal and/or biomass burning was important sources of PAHs in winter. Spring samples were clustered into Groups 3 and 4, characterized by Bb+jF, BeP, IcdP, and BghiP (Fig. 4c). BeP is generated from vehicles (He et al., 2020), and BghiP is also emitted from gasoline vehicles and tire treads (Larnesjö, 1999; Smith and Harrison, 1998). In addition, BbF and IcdP are related to oil combustion (Harrison et al., 1996; Ravindra et al., 2008). Some spring samples were grouped with the winter samples in Group 2 (Fig. 4c), denoting the influence of similar emission sources in both seasons. On the other hand, summer samples exhibited a scattered distribution across the score plot (Fig. 4b), suggesting that the sources of particulate PAHs in summer differ from those in winter and spring. In addition, some summer samples were clustered in Group 1 related to BkF, which is generally emitted from coal combustion (Ravindra et al., 2008). In summer, prevailing easterly winds (Fig. S3) may have transported PAHs emitted from the petrochemical and

nonferrous industrial complexes, where large amounts of coal and heavy oil are consumed, to the urban areas in Ulsan (Nguyen et al., 2018). The PCA result aligns with that of diagnostic ratios, indicating the dominance of pyrogenic sources (e.g., petroleum, coal, and biomass burning) in spring and the presence of both pyrogenic and petrogenic sources in summer (Fig. 5b).

3.2.2 Potential source areas

The CWT of Σ_{21} PAHs and BaP in the particulate phase was employed to identify potential source areas of PAHs (Fig. 6). Gaseous PAHs were not considered in the CWT analysis as they are known to be more influenced by local emissions (Kim et al., 2012; Nguyen et al., 2022). The CWT results revealed that during winter, the primary source regions for transported PAHs to Ulsan were northeast provinces in China (i.e., Heilongjiang, Jilin, and Liaoning) and the Korean Peninsula. Notably, on February 17, a significant increase in the BeP/BaP ratio was observed (Fig. S4). The higher BeP/BaP ratio suggests the LRAT of PAHs due to the faster decomposition of BaP compared to BeP, driven by photochemical reactions (Lee et al., 2011; Thang et al., 2019). Northeasterly winds prevailed on February 17 (Fig. S4), with an air mass originating from Mongolia arriving in Ulsan via China, North Korea, and the East Sea (Fig. S5a). This air mass did not pass over South Korea, emphasizing the greater influence of LRAT than local sources. Similarly, in spring, when the BeP/BaP ratio was high (April 1 and May 7) (Fig. S4), air masses were transported to the YN station bypassing South Korea (Fig. S5b). On the other hand, on days with high BeP/BaP ratios in summer (July 29 and August 13), air masses stayed over South Korea and surrounding seas (Fig. S5c). Furthermore, on June 24, unlike other summer

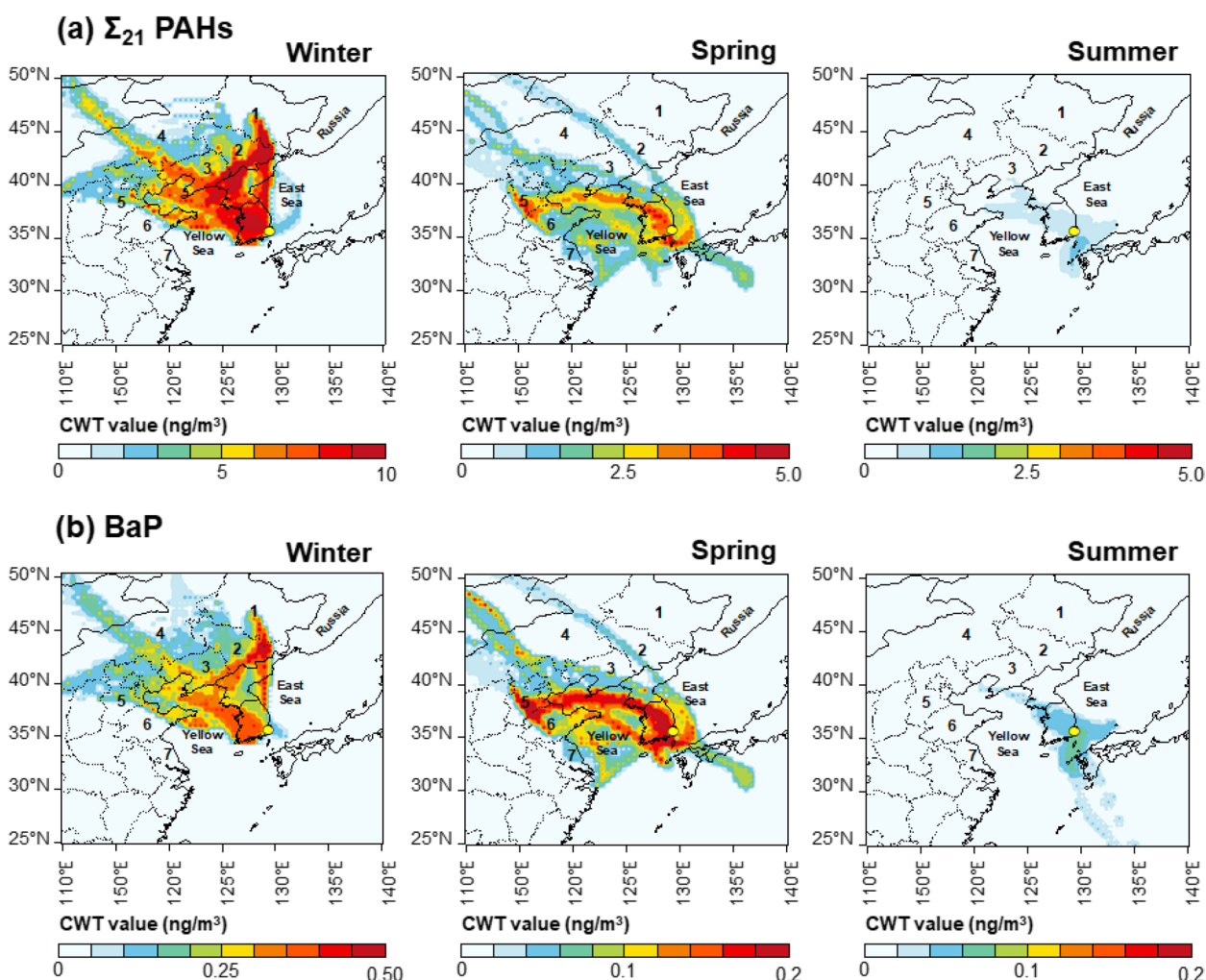


Fig. 6 Seasonal CWT results for **a** Σ_{21} PAHs and **b** BaP in the particulate phase. The numbers indicate several provinces in China: (1) Heilongjiang, (2) Jilin, (3) Liaoning, (4) Inner Mongolia, (5) Hebei, (6) Shandong, and (7) Jiangsu

days, the elevated BeP/BaP ratio was associated with air trajectories from eastern China. Despite no statistical seasonal difference (winter: 2.23 ± 1.53 , spring: 2.10 ± 1.04 , and summer: 1.79 ± 1.13 , Mann-Whitney rank-sum test, $p > 0.05$), the lowest value of the BeP/BaP ratio was found in summer, likely due to relatively low wind speeds amplifying the contribution of local sources. This result aligns with findings from a previous study (Nguyen et al., 2022). Therefore, the relative influence of LRAT and local pollution varied depending on the sampling date within each season.

In Table S6, BeP/BaP ratios in Ulsan were found to be similar to those observed in other cities across East Asia. In particular, the seasonal variation of the BeP/BaP ratio in Ulsan exhibited a trend comparable to that in Korean cities such as Gosan, Gwangju, and Daejeon. Unlike Seoul and Daesan, which are in closer proximity to China, these cities are relatively distant. The increased BeP/BaP ratio

in Ulsan might be influenced by the extended residence time of air parcels. Similarly, the BeP/BaP ratio in Japan showed a seasonal variation similar to that in Ulsan. In contrast, in China, BeP/BaP ratios were higher in summer compared to spring and winter. In addition, during winter and spring, air parcels reaching Ulsan traversed China and North Korea (Fig. S1), suggesting that the prolonged residence time of air parcels could contribute to an increased BeP/BaP ratio during the cold season.

3.3 Health risk assessment

The BaP_{eq} concentrations of total and individual PAHs in the gaseous, particulate, and total (gas + particle) phases are presented in Figs. S6 and S7, respectively. The total (gas + particle) concentration of Σ_{19} BaP_{eq} was highest in winter (mean: 0.60 ng/m^3), followed by spring (mean: 0.27 ng/m^3) and summer (mean: 0.17 ng/m^3). This result is primarily attributed to the higher PAH concentrations

in winter as described in Section 3.1 and the greater TEF values of dominant species in winter (i.e., 4- to 6-ring PAHs). The concentrations of particulate Σ_{19} BaP_{eq} were 3.5–17 times higher than those of gaseous PAHs due to the higher TEF values of particulate species (e.g., BaP, BkF, and BghiP). These BaP_{eq} levels are comparable to those in urban areas and lower than those in semirural and industrial areas in Ulsan (Nguyen et al., 2020). In addition, the concentration of Σ_{13} BaP_{eq} in Ulsan is generally lower than those reported in an industrial area in Taiwan (Liu et al., 2010) and urban areas in Beijing and Tenjin, China (Chao et al., 2019; Han et al., 2016).

The six non-US EPA priority PAHs (i.e., B_jF, DMBA, 3MCA, DbaiP, DbahP, and DbaP) made significant contributions to Σ_{19} BaP_{eq} concentrations, accounting for 21%, 19%, and 36% during winter, spring, and summer, respectively (Fig. S7b). Previous studies also highlighted the substantial contributions of these non-US EPA priority PAHs to total BaP_{eq}. For instance, dibenzopyrenes (e.g., DbaiP, DbahP, DbaP, and dibenzo[a,e]pyrene (DbaeP)) have been reported to contribute 52% of the risk of particulate Σ_{32} BaP_{eq} (Layshock et al., 2010; Wang et al., 2016). In another study, they also account for 28% of the total Σ_{53} BaP_{eq} concentration despite comprising only 0.8% of the Σ_{53} PAH concentration (Hong et al., 2020). Therefore, considering non-US EPA priority PAHs is crucial for evaluating human health risks.

The ILCR for the adult group (18–70 years old) through inhalation of the total (gas + particle) PAHs is illustrated in Fig. 7. The ranges of cancer risks for Σ_{13} PAHs were 4.73×10^{-9} – 5.00×10^{-7} in winter, 3.00×10^{-9} – 2.13×10^{-7} in spring, and 1.27×10^{-9} – 9.06×10^{-8} in summer (Fig. 7a). Additionally, the cancer risks for Σ_{21} PAHs were 7.51×10^{-9} – 6.43×10^{-7} in winter, 5.57×10^{-9} – 2.51

$\times 10^{-7}$ in spring, and 1.76×10^{-9} – 1.77×10^{-7} in summer (Fig. 7b). This seasonal trend (i.e., higher cancer risks in winter and spring) was consistent with that of a previous study in Ulsan (Nguyen et al., 2020). As the same risk parameters were used for the risk calculation for three seasons, the higher risks in winter and spring are due to greater PAH concentrations, particularly the 5- and 6-ring species having higher TEF values. Notably, both cancer risks of Σ_{13} and Σ_{19} PAHs were lower than the acceptable risk level (i.e., 10^{-6}) suggested by the US EPA, indicating no significant risk concerns related to inhalation of these PAHs in Ulsan. However, ILCRs of the total Σ_{19} PAHs were 1.2 to 1.6 times higher than those of Σ_{13} PAHs due to non-US EPA priority PAHs (e.g., DbaiP and DbahP) with high TEQs. Exposure to these species may affect human health because of their high toxicities (Hong et al., 2020; Layshock et al., 2010).

4 Conclusion

In this study, typical seasonal variations and phase distributions of 21 PAHs were observed in Ulsan, South Korea. The highest PAH levels were observed in winter, while the lowest levels were noted in summer. The 3- and 4-ring species were dominant in the gaseous phase, whereas 4-, 5-, and 6-ring PAHs were dominant in the particulate phase. During spring and summer, PAHs were mainly derived from gasoline and coal combustion. In particular, summer samples exhibited frequent influence from prevailing easterly winds and transporting PAHs emitted by the petrochemical and nonferrous industrial complexes. In winter, the impact of diesel and solid fuel combustion increased. In addition, the main source regions for the LRAT of PAHs to Ulsan were identified as the northeastern provinces of

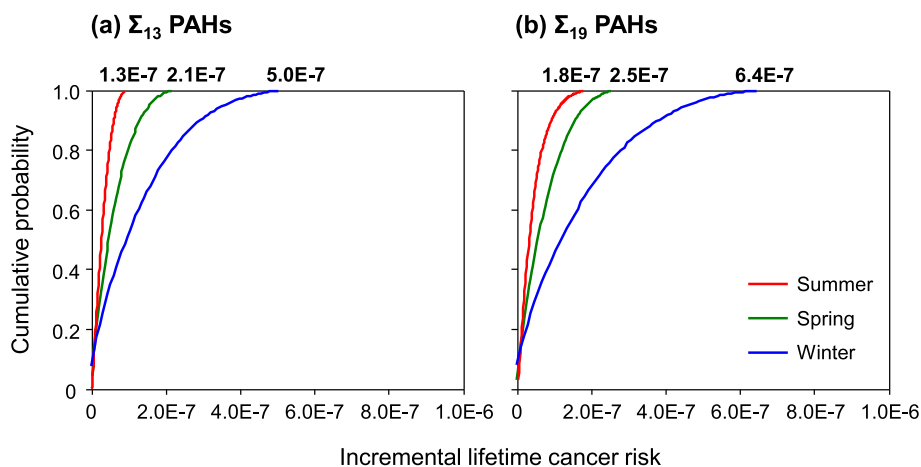


Fig. 7 Cumulative probability of ILCRs for **a** Σ_{13} PAHs and **b** Σ_{19} PAHs through inhalation. The maximum cancer risks are indicated for each seasonal line

China. The contribution of eight non-US EPA priority PAHs to the concentration of Σ_{21} PAHs was found to be 5.2%. However, their TEQs and cancer risks accounted for 23.3% and 20.0%, respectively, of those of Σ_{19} PAHs, particularly due to contributions from DbahP and DbahP. The results of this study suggest that human health risks may be underestimated when analyzing only the US EPA priority PAHs, emphasizing the need to focus on other toxic PAHs for a more comprehensive understanding of health risks.

Supplementary Information

The online version contains supplementary material available at <https://doi.org/10.1007/s44273-024-00032-1>.

Supplementary Material 1: Figure S1. Backward air trajectories arriving in Ulsan, South Korea. The red point presents the sampling site. **Figure S2.** Monthly and seasonal variations of (a) concentrations and (b) phase distributions of Σ_{21} PAHs. **Figure S3.** Wind fields and wind roses for winter, spring, and summer in Ulsan. The red dot and yellow arrow indicate the sampling site and prevailing wind directions, respectively. **Figure S4.** Temporal variations of BeP/BaP ratios and the concentrations of Σ_{21} PAHs in the particulate phase. The daily wind patterns are also presented. **Figure S5.** Density of backward air trajectories and daily trajectories with high BeP/BaP ratios in (a) winter, (b) spring, and (c) summer. The daily trajectory was calculated as the average of the hourly trajectories. **Figure S6.** Seasonal mean concentrations of BaPeq: (a) phase distributions of Σ_{19} BaPeq and (b) distributions of Σ_6 BaPeq (for non-US EPA priority compounds) and Σ_{13} BaPeq (for US EPA priority compounds) in the total (gas + particle) phase. **Figure S7.** Seasonal mean BaPeq concentrations of individual PAHs in the (a) gaseous, (b) particulate, and (c) total (gas + particle) phases over the study period. **Table S1.** MDLs and detection frequencies of the 21 target PAHs. **Table S2.** Names, abbreviations, IARC classifications, and TEF values of the target 21 PAHs. **Table S3.** Input data of Monte Carlo simulation to estimate cancer risk through inhalation. **Table S4.** Comparison of the concentrations of total Σ_{21} PAHs and US EPA Σ_{13} PAHs between this study and previous studies. **Table S5.** Spearman correlations among gaseous and particulate PAHs, TSP, PM₁₀, and PM_{2.5} during three sampling seasons. **Table S6.** Comparison of BeP/BaP ratios from selected Asian countries.

Authors' contributions

NRJ, writing — original draft, formal analysis, and data curation. S-JL, writing — review and editing and formal analysis. TNTN, writing — review and editing. H-YL, formal analysis. HKC, formal analysis. C-KS, supervision. S-DC, supervision, writing — review and editing, and project administration.

Funding

This research was supported by the National Research Foundation of Korea (NRF) grant funded by the Korean government (2020R1A6A1A03040570, RS-2023-00209329). It was also supported by a grant from the National Institute of Environment Research (NIER), funded by the Ministry of Environment (MOE) of the Republic of Korea (NIER-2021-03-03-007).

Availability of data and materials

The datasets used and/or analyzed during the current study are available from the corresponding author on reasonable request.

Declarations

Ethics approval and consent to participate

Not applicable.

Consent for publication

Not applicable.

Competing interests

The authors declare that they have no competing interests.

Author details

¹Department of Civil, Urban, Earth, and Environmental Engineering, Ulsan National Institute of Science and Technology (UNIST), Ulsan 44919, Republic of Korea. ²Faculty of Environmental Sciences, Saigon University, Ho Chi Minh City 74900, Vietnam. ³Research and Management Center for Particulate Matter in the Southeast Region of Korea, Ulsan National Institute of Science and Technology (UNIST), Ulsan 44919, Republic of Korea.

Received: 4 December 2023 Accepted: 31 March 2024

Published online: 16 April 2024

References

- Akyuz, M., & Cabuk, H. (2010). Gas-particle partitioning and seasonal variation of polycyclic aromatic hydrocarbons in the atmosphere of Zonguldak, Turkey. *Science of the Total Environment*, *408*, 5550–5558.
- Andersson, J. T., & Achten, C. (2015). Time to say goodbye to the 16 EPA PAHs? Toward an up-to-date use of PACs for environmental purposes. *Polycyclic Aromatic Compounds*, *35*, 330–354.
- Andrade, S. J. D., Cristale, J., Silva, F. S., Julião Zocolo, G., & Marchi, M. R. R. (2010). Contribution of sugar-cane harvesting season to atmospheric contamination by polycyclic aromatic hydrocarbons (PAHs) in Araraquara city, Southeast Brazil. *Atmospheric Environment*, *44*, 2913–2919.
- Baek, S. O., Field, R. A., Goldstone, M. E., Kirk, P. W., Lester, J. N., & Perry, R. (1991). A review of atmospheric polycyclic aromatic hydrocarbons: Sources, fate and behavior. *Water, Air, & Soil Pollution*, *60*, 279–300.
- Baek, K.-M., Kim, M.-J., Kim, J.-Y., Seo, Y.-K., & Baek, S.-O. (2020). Characterization and health impact assessment of hazardous air pollutants in residential areas near a large iron-steel industrial complex in Korea. *Atmospheric Pollution Research*, *11*, 1754–1766.
- Baek, K.-M., Kim, M.-J., Seo, Y.-K., Kang, B.-W., Kim, J.-H., & Baek, S.-O. (2020). Spatiotemporal variations and health implications of hazardous air pollutants in Ulsan, a multi-industrial city in Korea. *Atmosphere*, *11*, 547.
- Baek, K.-M., Seo, Y.-K., Kim, J.-Y., & Baek, S.-O. (2020). Monitoring of particulate hazardous air pollutants and affecting factors in the largest industrial area in South Korea: The Sihwa-Banwol complex. *Environmental Engineering Research*, *25*, 908–923.
- Chao, S., Liu, J., Chen, Y., Cao, H., & Zhang, A. (2019). Implications of seasonal control of PM_{2.5}-bound PAHs: An integrated approach for source apportionment, source region identification and health risk assessment. *Environmental Pollution*, *247*, 685–695.
- Chen, Y., Li, X., Zhu, T., Han, Y., & Lv, D. (2017). PM_{2.5}-bound PAHs in three indoor and one outdoor air in Beijing: Concentration, source and health risk assessment. *Science of the Total Environment*, *586*, 255–264.
- Cheruiyot, N. K., Lee, W.-J., Mwangi, J. K., Wang, L.-C., Lin, N.-H., Lin, Y.-C., Cao, J., Zhang, R., & Chang-Chien, G.-P. (2015). An overview: Polycyclic aromatic hydrocarbon emissions from the stationary and mobile sources and in the ambient air. *Aerosol and Air Quality Research*, *15*, 2730–2762.
- Choi, S.-D., Ghim, Y. S., Lee, J. Y., Kim, J. Y., & Kim, Y. P. (2012). Factors affecting the level and pattern of polycyclic aromatic hydrocarbons (PAHs) at Gosan, Korea during a dust period. *Journal of Hazardous Materials*, *227–228*, 79–87.
- Choi, S.-D., Kwon, H.-O., Lee, Y.-S., Park, E.-J., & Oh, J.-Y. (2012). Improving the spatial resolution of atmospheric polycyclic aromatic hydrocarbons using passive air samplers in a multi-industrial city. *Journal of Hazardous Materials*, *241*, 252–258.
- Collins, J. F., Brown, J. P., Alexeeff, G. V., & Salmon, A. G. (1998). Potency equivalency factors for some polycyclic aromatic hydrocarbons and polycyclic aromatic hydrocarbon derivatives. *Regulatory Toxicology and Pharmacology*, *28*, 45–54.
- US EPA. (1993). Provisional guidance for quantitative risk assessment of polycyclic aromatic hydrocarbons, United States Environmental Protection Agency.
- Esen, F., Tasdemir, Y., & Vardar, N. (2008). Atmospheric concentrations of PAHs, their possible sources and gas-to-particle partitioning at a residential site of Bursa, Turkey. *Atmospheric Research*, *88*, 243–255.

- Han, B., Liu, Y., You, Y., Xu, J., Zhou, J., Zhang, J., Niu, C., Zhang, N., He, F., Ding, X., & Bai, Z. (2016). Assessing the inhalation cancer risk of particulate matter bound polycyclic aromatic hydrocarbons (PAHs) for the elderly in a retirement community of a mega city in North China. *Environmental Science and Pollution Research*, 23, 20194–20204.
- Harkov, R., & Greenberg, A. (1985). Benzo(a)pyrene in New Jersey-Results from a twenty-seven-site study. *Journal of the Air Pollution Control Association*, 35, 238–243.
- Harrison, R. M., Smith, D., & Luhana, L. (1996). Source apportionment of atmospheric polycyclic aromatic hydrocarbons collected from an urban location in Birmingham, UK. *Environmental Science & Technology*, 30, 825–832.
- He, Y., He, W., Yang, C., Liu, W., & Xu, F. (2020). Spatiotemporal toxicity assessment of suspended particulate matter (SPM)-bound polycyclic aromatic hydrocarbons (PAHs) in Lake Chaohu, China: Application of a source-based quantitative method. *Science of the Total Environment*, 727, 138690.
- Hong, W. J., Jia, H., Yang, M., & Li, Y. F. (2020). Distribution, seasonal trends, and lung cancer risk of atmospheric polycyclic aromatic hydrocarbons in North China: A three-year case study in Dalian city. *Ecotoxicological Environmental Safety*, 196, 110526.
- Hong, W.-J., Dong, W.-J., Zhao, T.-T., Zheng, J.-Z., Lu, Z.-G., Ye, C., (2023). Ambient PM_{2.5}-bound polycyclic aromatic hydrocarbons in Ningbo Harbor, eastern China: Seasonal variation, source apportionment, and cancer risk assessment. *Air Quality, Atmosphere & Health*, 16, 1809–1821.
- Hsu, Y.-K., Holsen, T. M., & Hopke, P. K. (2003). Comparison of hybrid receptor models to locate PCB sources in Chicago. *Atmospheric Environment*, 37, 545–562.
- Hsu, Y.-M., Harner, T., Li, H., & Fellin, P. (2015). PAH measurements in air in the athabasca oil sands region. *Environmental Science & Technology*, 49, 5584–5592.
- IARC. (2010). IARC monographs on the evaluation of carcinogenic risks to humans, in: Lyon, F. (Ed.), Some non-heterocyclic polycyclic aromatic hydrocarbons and some related exposures. International Agency for Research on Cancer.
- Ichikawa, Y., Watanabe, T., Horimoto, Y., Ishii, K., & Naito, S. (2018). Measurements of 50 non-polar organic compounds including polycyclic aromatic hydrocarbons, n-alkanes and phthalate esters in fine particulate matter (PM_{2.5}) in an industrial area of chiba prefecture, Japan. *Asian Journal of Atmospheric Environment*, 12, 274–288.
- Kim, J., Lee, J., Kim, Y., Lee, S.-B., Jin, H., & Bae, G.-N. (2012). Seasonal characteristics of the gaseous and particulate PAHs at a roadside station in Seoul, Korea. *Atmospheric Research*, 116, 142–150.
- Kim, M.-J., Baek, K.-M., Heo, J.-B., Cheong, J.-P., & Baek, S.-O. (2021). Concentrations, health risks, and sources of hazardous air pollutants in Seoul-Incheon, a megacity area in Korea. *Air Quality, Atmosphere & Health*, 14, 873–893.
- Kirchsteiger, B., Materić, D., Happenhofer, F., Holzinger, R., Kasper-Giebl, A., (2023). Fine micro-and nanoplastics particles (PM_{2.5}) in urban air and their relation to polycyclic aromatic hydrocarbons. *Atmospheric Environment*, 301, 119670.
- Kiss, G., Varga-Puchony, Z., Rohrbacher, G., & Hlavay, J. (1998). Distribution of polycyclic aromatic hydrocarbons on atmospheric aerosol particles of different sizes. *Atmospheric Research*, 46, 153–261.
- Kulkarni, P., & Venkataraman, C. (2000). Atmospheric polycyclic aromatic hydrocarbons in Mumbai, India. *Atmospheric Environment*, 34, 2785–2790.
- Kwon, H.-O., & Choi, S.-D. (2014). Polycyclic aromatic hydrocarbons (PAHs) in soils from a multi-industrial city, South Korea. *Science of the Total Environment*, 470–471, 1494–1501.
- Larnesjö, P. (1999). *Applications of source receptor models using air pollution data in Stockholm*. Stockholms universitet.
- Layshock, J., Simonich, S. M., & Anderson, K. A. (2010). Effect of dibenzopyrene measurement on assessing air quality in Beijing air and possible implications for human health. *Journal of Environmental Monitoring*, 12, 2290–2298.
- Lee, J. Y., Kim, Y. P., & Kang, C.-H. (2011). Characteristics of the ambient particulate PAHs at Seoul, a mega city of Northeast Asia in comparison with the characteristics of a background site. *Atmospheric Research*, 99, 50–56.
- Lee, Y.-K., Lee, J.-H., Beak, N.-G., Kim, K.-C., & Han, J.-S. (2023). Seasonal and emission characteristics of PAHs in the ambient air of industrial complexes. *Atmosphere*, 15, 30.
- Lee, S.-J., Lee, H.-Y., Kim, S.-J., Kang, H.-J., Kim, H., Seo, Y.-K., Shin, H.-J., Ghim, Y.S., Song, C.-K., Choi, S.-D., 2023a. Pollution characteristics of PM_{2.5} during high concentration periods in summer and winter in Ulsan, the largest industrial city in South Korea. *Atmospheric Environment*, 292, 119418.
- Liu, H. H., Yang, H. H., Chou, C. D., Lin, M. H., & Chen, H. L. (2010). Risk assessment of gaseous/particulate phase PAH exposure in foundry industry. *Journal of Hazardous Materials*, 181, 105–111.
- Liu, D., Xu, Y., Chaemfa, C., Tian, C., Li, J., Luo, C., & Zhang, G. (2014). Concentrations, seasonal variations, and outflow of atmospheric polycyclic aromatic hydrocarbons (PAHs) at Ningbo site, eastern China. *Atmospheric Pollution Research*, 5, 203–209.
- Masala, S., Lim, H., Bergvall, C., Johansson, C., & Westerholm, R. (2016). Determination of semi-volatile and particle-associated polycyclic aromatic hydrocarbons in Stockholm air with emphasis on the highly carcinogenic dibenzopyrene isomers. *Atmospheric Environment*, 140, 370–380.
- Mostert, M. M. R., Ayoko, G. A., & Kokot, S. (2010). Application of chemometrics to analysis of soil pollutants. *TRAC Trends in Analytical Chemistry*, 29, 430–445.
- Nguyen, T. N. T., Jung, K.-S., Son, J. M., Kwon, H.-O., & Choi, S.-D. (2018). Seasonal variation, phase distribution, and source identification of atmospheric polycyclic aromatic hydrocarbons at a semi-rural site in Ulsan, South Korea. *Environmental Pollution*, 236, 529–539.
- Nguyen, T. N. T., Kwon, H.-O., Lammel, G., Jung, K.-S., Lee, S.-J., & Choi, S.-D. (2020). Spatially high-resolved monitoring and risk assessment of polycyclic aromatic hydrocarbons in an industrial city. *Journal of Hazardous Materials*, 393, 122409.
- Nguyen, T. N. T., Vuong, Q. T., Lee, S.-J., Xiao, H., & Choi, S.-D. (2022). Identification of source areas of polycyclic aromatic hydrocarbons in Ulsan, South Korea, using hybrid receptor models and the conditional bivariate probability function. *Environmental Science: Processes & Impacts*, 24, 140–151.
- NIER. (2016). Monitoring of hazardous air pollutants in the industrial ambient atmosphere (II). National Institute of Environmental Research.
- NIER. (2018). Monitoring of hazardous air pollutants in the urban ambient atmosphere (IV). National Institute of Environmental Research.
- NIER. (2019). Monitoring of hazardous air pollutants in the urban ambient atmosphere (V). National Institute of Environmental Research.
- Nisbet, I. C. T., & Lagoy, P. K. (1992). Toxic equivalency factors (TEFs) for polycyclic aromatic hydrocarbons (PAHs). *Regulatory Toxicology and Pharmacology*, 16, 290–300.
- OEHHA. (1994). Benzo[a]pyrene as a toxic air contaminant. Office of Environmental Health Hazard Assessment.
- Ravindra, K., Sokhi, R., & Vangrieken, R. (2008). Atmospheric polycyclic aromatic hydrocarbons: Source attribution, emission factors and regulation. *Atmospheric Environment*, 42, 2895–2921.
- Ray, D., Ghosh, A., Chatterjee, A., Ghosh, S. K., & Raha, S. (2019). Size-specific PAHs and associated health risks over a tropical urban metropolis: Role of long-range transport and meteorology. *Aerosol and Air Quality Research*, 19, 2446–2463.
- Silva, D. A., & Bicego, M. C. (2010). Polycyclic aromatic hydrocarbons and petroleum biomarkers in São Sebastião Channel, Brazil: Assessment of petroleum contamination. *Marine Environmental Research*, 69, 277–286.
- Simcik, M. F., Eisenreich, S. J., & Liroy, P. J. (1999). Source apportionment and source/sink relationships of PAHs in the coastal atmosphere of Chicago and Lake Michigan. *Atmospheric Environment*, 33, 5071–5079.
- Smith, D., & Harrison, R. (1998). Polycyclic aromatic hydrocarbons in atmospheric particles. *Atmospheric Particles*, 5, 253–294.
- Stojic, A., & Stojic, S. S. (2017). The innovative concept of three-dimensional hybrid receptor modeling. *Atmospheric Environment*, 164, 216–223.
- Sun, J.-L., Jing, X., Chang, W.-J., Chen, Z.-X., & Zeng, H. (2015). Cumulative health risk assessment of halogenated and parent polycyclic aromatic hydrocarbons associated with particulate matters in urban air. *Ecotoxicology and Environmental Safety*, 113, 31–37.
- Tang, N., Hattori, T., Taga, R., Igarashi, K., Yang, X., Tamura, K., Kakimoto, H., Mishukov, V. F., Toriba, A., & Kizu, R. (2005). Polycyclic aromatic hydrocarbons and nitropolycyclic aromatic hydrocarbons in urban air particulates and their relationship to emission sources in the Pan-Japan Sea countries. *Atmospheric Environment*, 39, 5817–5826.
- Thang, P. Q., Kim, S.-J., Lee, S.-J., Ye, J., Seo, Y.-K., Baek, S.-O., & Choi, S.-D. (2019). Seasonal characteristics of particulate polycyclic aromatic hydrocarbons (PAHs) in a petrochemical and oil refinery industrial area on the west coast of South Korea. *Atmospheric Environment*, 198, 398–406.
- Vuong, Q. T., Thang, P. Q., Nguyen, T. N. T., Ohura, T., & Choi, S.-D. (2020). Seasonal variation and gas/particle partitioning of atmospheric halogenated

- polycyclic aromatic hydrocarbons and the effects of meteorological conditions in Ulsan, South Korea. *Environmental Pollution*, 263, 114592.
- Wang, Y. Q., Zhang, X. Y., & Draxler, R. R. (2009). TrajStat: GIS-based software that uses various trajectory statistical analysis methods to identify potential sources from long-term air pollution measurement data. *Environmental Modelling & Software*, 24, 938–939.
- Wang, Q., Kobayashi, K., Lu, S., Nakajima, D., Wang, W., Zhang, W., Sekiguchi, K., & Terasaki, M. (2016). Studies on size distribution and health risk of 37 species of polycyclic aromatic hydrocarbons associated with fine particulate matter collected in the atmosphere of a suburban area of Shanghai city, China. *Environmental Pollution*, 214, 149–160.
- Yunker, M. B., Macdonald, R. W., Vingarzan, R., Mitchell, R. H., Goyette, D., Sylvestre, S. (2002). PAHs in the Fraser River basin: a critical appraisal of PAH ratios as indicators of PAH source and composition. *Organic Geochemistry*, 33, 489–515.

Publisher's Note

Springer Nature remains neutral with regard to jurisdictional claims in published maps and institutional affiliations.